

Primljen / Received: 17.11.2020.

Ispravljen / Corrected: 15.3.2021.

Prihvaćen / Accepted: 4.8.2021.

Dostupno online / Available online: 10.10.2021.

Evaluation of masonry buildings and mosques after Sivrice earthquake

Authors:



Assist.Prof. **Halit Cenan Mertol**, PhD. CE
Atilim University, Ankara, Turkey
Civil Engineering Department
cenan.mertol@atilim.edu.tr
Corresponding author



Assist.Prof. **Gokhan Tunc**, PhD. CE
Atilim University, Ankara, Turkey
Civil Engineering Department
gokhan.tunc@atilim.edu.tr



Prof. **Tolga Akis**, PhD. CE
Atilim University, Ankara, Turkey
Civil Engineering Department
tolga.akis@atilim.edu.tr

Research Paper

Halit Cenan Mertol, Gokhan Tunc, Tolga Akis

Evaluation of masonry buildings and mosques after Sivrice earthquake

The evaluation of masonry and mosque type structures after the Sivrice Earthquake is presented in this study. Stone masonry buildings exhibited damage such as vertical cracks and splitting at corners, wedge shaped corner failures, diagonal cracking on walls, out-of-plane splitting of walls, and separation of walls from flooring/roofing systems. On the other hand, the separation of flags and caps of minarets was a common example of damage in mosques. Future earthquake damage can be prevented by following design codes and providing adequate supervision for new structures, while strengthening measures are recommended for the existing buildings.

Key words:

Sivrice earthquake, hazard, structural damage, masonry building, mosque, strengthening

Prethodno priopćenje

Halit Cenan Mertol, Gokhan Tunc, Tolga Akis

Procjena stanja zidanih građevina i džamija nakon potresa u Sivricu

U radu je prikazana procjena stanja zidanih građevina i džamija nakon potresa u gradu Sivricu u Turskoj. Zidane kamene građevine pretrpjele su razna oštećenja kao što su pojava vertikalnih pukotina i razdvajanja u kutovima, klinasta popuštanja u kutovima, otvaranje dijagonalnih pukotina na zidovima, otkazivanje zidova izvan ravnine i odvajanje zidova od katnih ili krovnih sustava. S druge strane, odvajanje stošca i alema minareta karakterističan je primjer oštećenja džamija. Buduća oštećenja izazvana potresom mogu se spriječiti primjerenim poštivanjem propisa o projektiranju i odgovarajućim nadzorom tijekom građenja novih građevina, dok se za postojeće građevine preporučuju prikladne mjere pojačanja.

Ključne riječi:

potres u Sivricu, opasnost, oštećenje konstrukcije, zidana građevina, džamija, pojačanje

1. Introduction

Turkey is located in one of the most active earthquake zones. According to statistical studies, a strong earthquake (with a magnitude, M_w , from 6.0 to 6.9) occurs every two years, and a major one (with a magnitude, M_w , above 6.9) occurs every three years. There are several fault lines that generate strong earthquakes. These are mainly the North Anatolian Fault Line (NAF), the East Anatolian Fault Line (EAF), and the West Anatolian Fault Lines (WAF) (Figure 1). In the northern part of Turkey, the NAF extends close to 1,500 km in length, and spans east to west. In the east and southeastern parts of the country, the EAF extends from the Gulf of Iskenderun to the city of Hakkari, assuming the shape of an arc. In the western part of the country, the WAF covers an area encircled by the Bakırçay, Gediz, Küçük, and Büyük Menderes rift valleys. The town of Sivrice, in Elazığ province, located in the eastern part of Turkey, suffered from a strong earthquake with a magnitude of $M_w = 6.8$ on 24 January 2020 [2]. The hypocentre was located 8.06 kilometres below the epicentre (close to Sivrice). This earthquake affected more than two million people living mainly in two cities, Elazığ and Malatya, and the surrounding towns and villages. Elazığ is located 37.5 km north-east and Malatya is located 65 km west of the epicentre of the earthquake. The location of the epicentre of the earthquake is shown in Figure 2. Forty-one people lost their lives during this earthquake and

hundreds were injured. More than 600 reinforced-concrete and masonry buildings collapsed and more than ten thousand buildings suffered from heavy damage. Over twenty thousand buildings experienced moderate or minor damage. In addition, more than 800 buildings were found to be structurally inadequate, and were demolished after the earthquake [3].

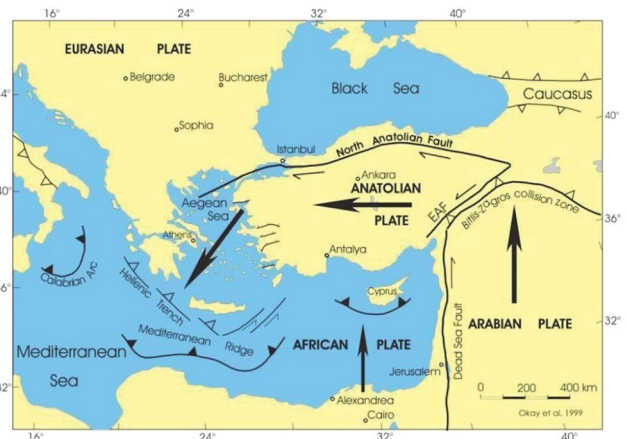


Figure 3. Intercontinental plate movement [4]

A reconnaissance team performed a technical visit to the earthquake-affected region within 24 hours after the earthquake. The observations and findings of this site visit, with respect to masonry buildings and mosques, are presented in this study.

2. Seismicity and tectonics

2.1. History

During the neotectonic period (approx. 12 million years BC), due to the collision of the larger Arabian and smaller Anatolian plates, plate movement began in the north-south direction [4]. The East Anatolian region is comprised of left-lateral strike slip types of faults, spanning from the city of Bingöl to Antakya, a town near the city of Hatay. This specific area and its associated fault lines is known as the East Anatolian Fault Zone (EAFZ or EAF) [5] (Figure 3). The annual slip rate of this fault zone is somewhere around 7.9 ± 0.3 mm [6]. The EAF covers a total distance of approximately 145 kilometres, starting from Lake Hazar (Elazığ) to Sincik (Adıyaman). It passes through Sivrice (Elazığ), Doğanöyl (Malatya), and continues to the Şilo Stream in Pütürge (Malatya) [7].



Figure 1. Active fault lines in Turkey [1]

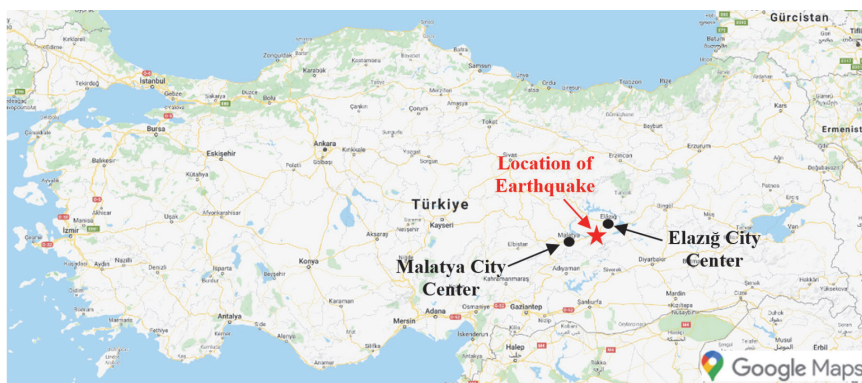


Figure 2. Location of Earthquake Epicentre (Sivrice)

2.2. Earthquake hazard map

The current Earthquake Hazard Map of Turkey, which was prepared based on earthquakes that have a 10 % exceedance probability in 50 years, or the equivalent, for a return period of 475 years, is shown in Figure 4 [8].

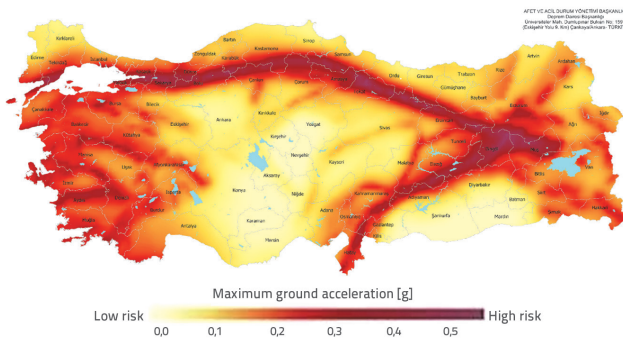


Figure 4. Earthquake Hazard Map of Turkey (probability of 10 % exceedance in 50 years) [8]

According to this map, the most severe earthquake regions are the northern, eastern and south-eastern parts of Turkey, the area near the Aegean Sea, and the inner southwestern part of Turkey, including the area surrounded by Lake Van. A more detailed hazard map of the central and eastern parts of Turkey, with expected earthquake ground motion acceleration values calculated based on 10 % exceedance in 50 years, is shown in Figure 5 [8]. Figure 6 shows the active fault lines in and around the epicentre of the Sivrice Earthquake, which lies on the EAF line [1]. Based on the data given in Figure 5 and Figure 6, the smallest and largest peak ground acceleration values in the Sivrice Earthquake region amount to 0.2 g and 0.8 g, respectively. Specifically, the average peak ground acceleration values in Sivrice and Doğanyol are both 0.63 g [8].

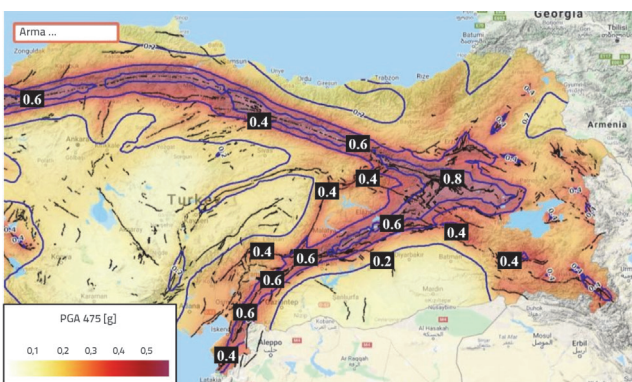


Figure 5. Expected peak ground acceleration values (in g) for earthquakes (probability of 10 % exceedance in 50 years) along the North and East Anatolian Fault Zones [8]

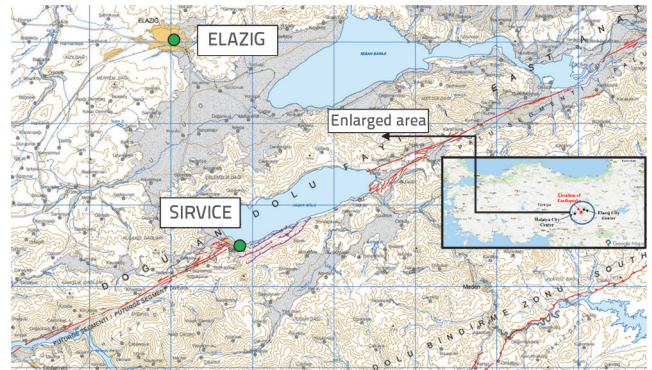


Figure 6. Active fault lines around Elazığ [1]

2.3. Sivrice earthquake

The Sivrice Earthquake occurred on 24 January 2020 at 8:55:11 p.m. local time [2]. The earthquake’s epicentre was Çevrimtaş, a village in Sivrice, which is located 37 kilometres in the north-western part of the city of Elazığ. The earthquake had a focal depth of 8.06 km, and its magnitude was $M_w=6.8$ [2]. The earthquake occurred in the Pütürge segment, which is a part of the East Anatolian Fault line characterized by a left lateral-strike slip-faulting mechanism. Based on various sources [9, 10], the earthquake created a surface rupture with an area of nearly 50 to 55 km². Although the earthquake did not cause a visible rupture on the surface, researchers surveying the area established by remote sensing methods a displacement of approximately 50 cm [9, 11]. The results from the moment tensor solution of the earthquake are given in Table 1.

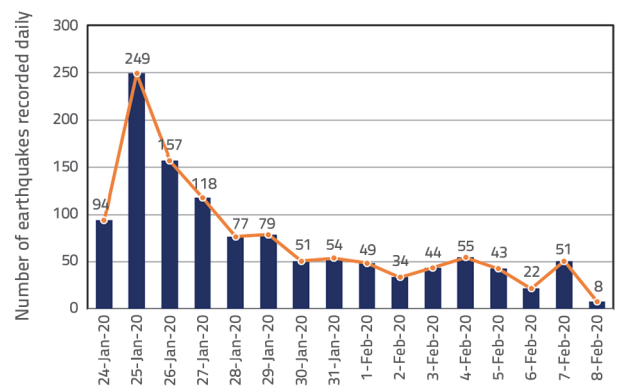



Figure 7. Total number of aftershocks recorded in the region between 24 January 2020 and 8 February 2020

Based on the earthquake data collected between 24 January 2020 and 8 February 2020 (16 days), a total of 1,185 aftershocks were

Table 1. Moment tensor solution of Sivrice, Elazığ Earthquake [2]

	Strike 1	Dip 1	Rake 1	Strike 2	Dip 2	Rake 2
		248	76	1	158	89

recorded in the area, with local magnitudes varying from 1.2 to 5.1. Figure 7 shows the daily frequency distribution of a total of 1,185 earthquakes following the main shock. In order to determine the characteristics of the aftershocks, the total number of aftershocks is also categorized according to their magnitudes (Table 2).

Table 2. Number of aftershocks categorized according to their local magnitudes (24 January 2020 to 8 February 2020)

Local magnitude	Number of aftershocks
$M_L \geq 5.0$	1
$5.0 > M_L \geq 4.0$	34
$4.0 > M_L \geq 3.0$	133
$3.0 > M_L \geq 2.0$	611
$M_L < 2.0$	406
Total	1185

Table 3 shows the peak ground acceleration values of the five nearest stations, obtained from AFAD's strong ground motion recording stations. The locations of these stations are also plotted on the map in Figure 8. Based on the data, the closest station was the Sivrice station (station number 2308), which was 24 kilometres away from the epicentre, while the most distant one was the Maden station (station number 2302), located 53 kilometres away from the epicentre. The maximum

ground acceleration recorded at the Sivrice station was in the East-West direction with a magnitude of 0.293 g.

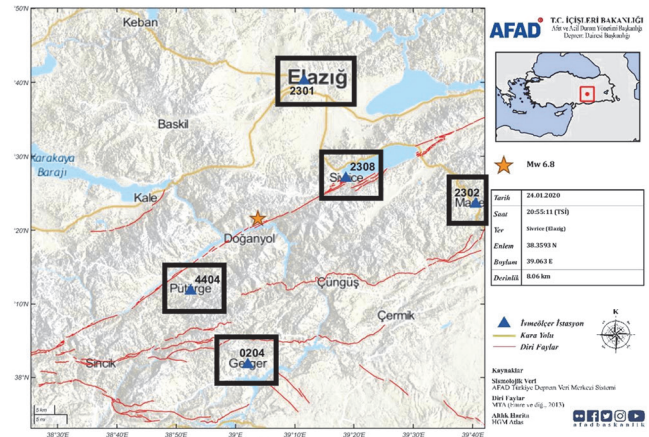


Figure 8. Locations of five closest strong ground motion recording stations [2]

2.4. Arias Intensity of the Sivrice Earthquake

Figure 9 shows the Arias Intensity (AI) of the Sivrice Earthquake for the N-S and E-W directions based on the ground motion data recorded at the Sivrice station. The effective duration of

Table 3. Earthquake data registered at five closest ground motion recording stations

No	Location		Station number	Latitude & longitude [°]	Peak ground acceleration values [Gal]			Shortest distance to the epicentre [km]
	City	Region			north-south	east-west	Vertical	
1	Elazığ	Sivrice	2308	38.4506 39.3102	237.99 (0.24 g)	292.77 (0.30 g)	190.09 (0.19 g)	24
2	Malatya	Pütürge	4404	38.1959 38.8738	206.91 (0.21 g)	239.24 (0.24 g)	153.87 (0.16 g)	25
3	Elazığ	Merkez	2301	38.6704 39.1927	119.28 (0.12 g)	140.73 (0.14 g)	66.31 (0.07 g)	36
4	Adıyaman	Gerger	0204	38.0290 39.0347	94.03 (0.10 g)	110.11 (0.11 g)	60.75 (0.06 g)	37
5	Elazığ	Maden	2302	38.3923 39.6754	26.29 (0.03 g)	33.97 (0.03 g)	22.78 (0.02 g)	53

1 Gal = 0.01 m/s². 1 g = 981 Gal

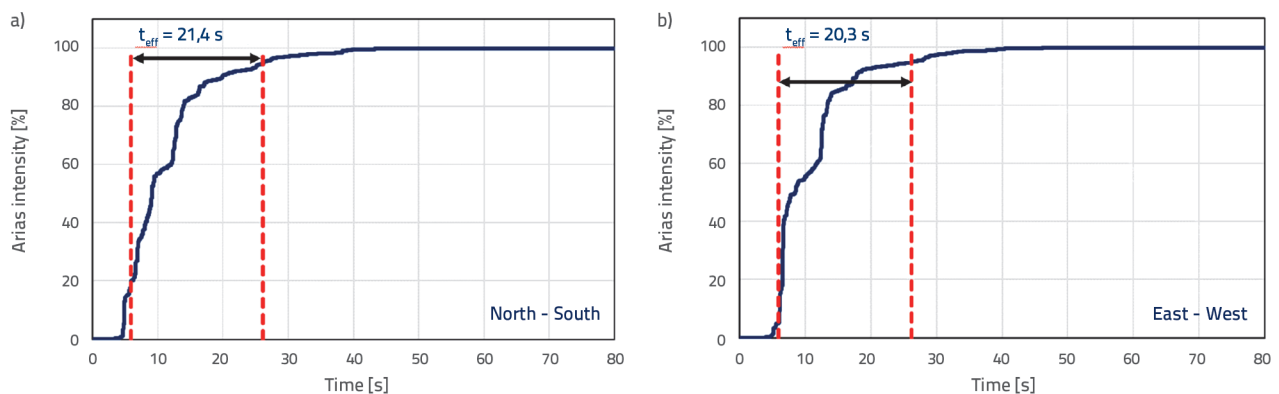


Figure 9. Effective duration of the Sivrice earthquake: a) North-South Direction; b) East-West Direction

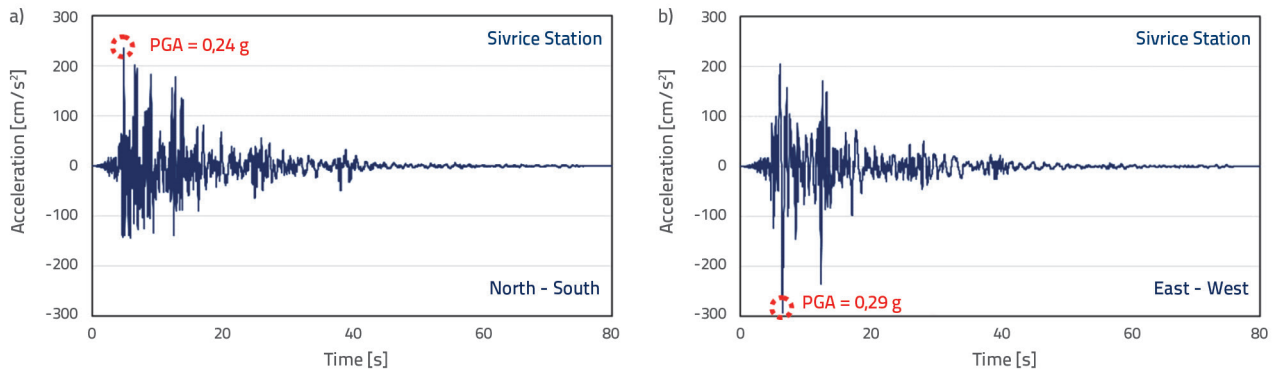


Figure 10. Peak ground accelerations for Sivrice earthquake: a) North-South Direction; b) East-West Direction

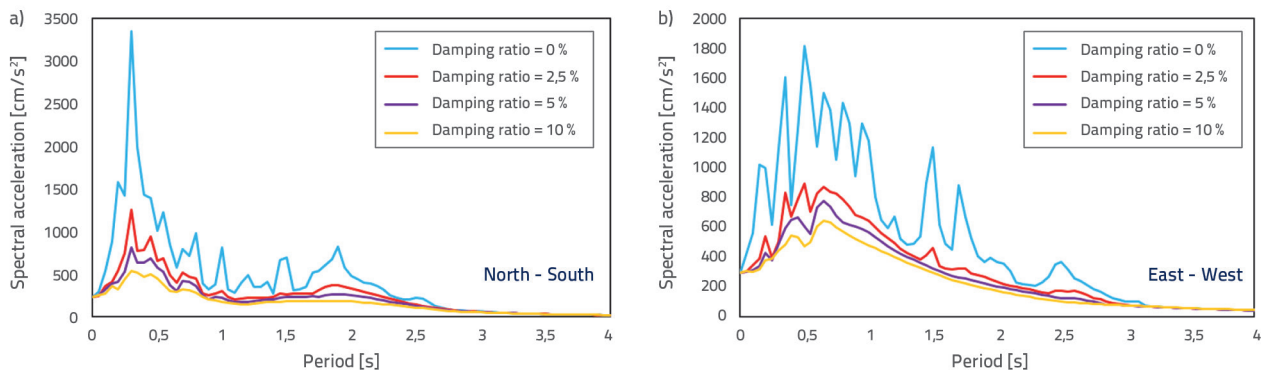


Figure 11. Spectral acceleration values for Sivrice earthquake: a) North-South Direction; b) East-West Direction

an earthquake is the time difference between the AI values of 5 % and 95 %. Based on the data plotted in Figure 9, the effective durations of the earthquake were determined as 21.4 seconds in the North-South direction, and 20.3 seconds in the East-West direction.

3. Evaluation of strong ground motion data

Figure 10 shows ground acceleration values for the Sivrice Earthquake, recorded at the Sivrice station, in both the North-South and East-West directions. According to the data, the peak ground acceleration values for the both directions are 0.24 g and 0.29 g, respectively. Spectral acceleration curves are

plotted using the peak ground acceleration values recorded at the Sivrice station in the North-South and East-West directions as a function of varying damping ratios (see Figure 11). The design spectrum curves from the current Turkish Building Earthquake Code (TBEC) [12] were compared to the spectral acceleration data plotted in Figure 12. TBEC [12] defines a total of 6 local soil classes, identified by letters ZA through ZF, where ZA denotes hard rock, and ZF denotes extremely loose soil, which needs further soil testing and site evaluation. In this study, the design spectrum curves of the first five soil types (excluding soil type ZF) were used to evaluate the North-South and East-West acceleration components of the Sivrice Earthquake. As illustrated in Figure 12, the East-West component of the

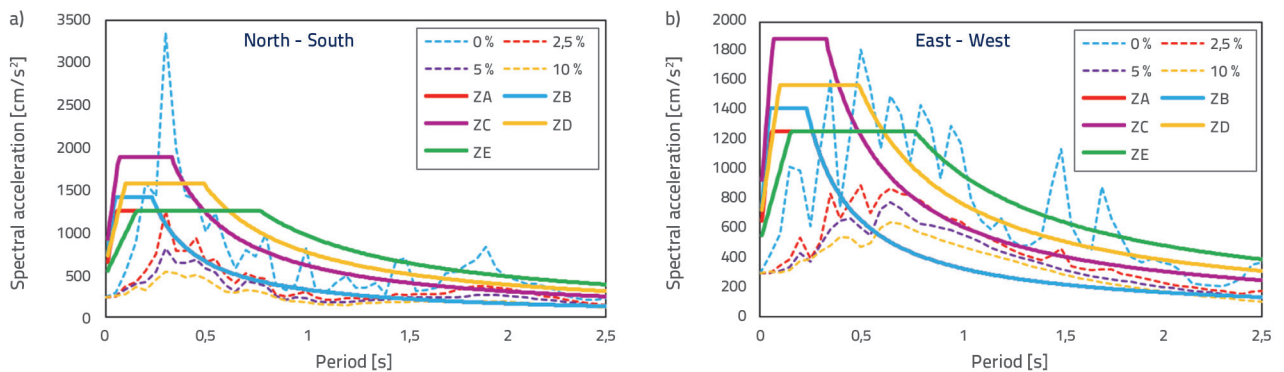


Figure 12. Spectral acceleration and design spectrum values for Sivrice earthquake: a) North-South Direction; b) East-West Direction

earthquake had a slightly greater impact on buildings located specifically in local soil classes ZC, ZD and ZE, with a period greater than 0.5 seconds compared to its North-South component. This points to the impact of site on the earthquake ground motion.

According to MTA, local soil conditions at the Sivrice station are defined as gabbro type of rock [13]. Gabbro is a coarse-grained and usually dark-colored igneous rock, typical for soil classes between ZB and ZC. However, there are four distinct types of soil in the close proximity of the station, which are undifferentiated quaternary, clastic and carbonate rocks, undifferentiated continental clastic rocks, and alluvial soil and sediments (ZC, ZD, ZE and ZF). The impact of soil can be seen from the increase that occurred both in the N-S and specifically in the E-W Sivrice spectra beyond 1.5 seconds (see Figure 12a-b). This increase is believed to negatively influence buildings by moving them into inelastic excursions in a 1.5 to 2 second period range. Therefore, it can be concluded that local soil conditions played an important role in altering the ground acceleration pattern.

4. Damage to masonry buildings

Numerous villages and towns were visited to evaluate performance of masonry buildings affected by the earthquake. Typical masonry buildings constructed in the villages and counties of the region are shown in Figure 13. The construction of some of these masonry buildings dates back to the 1950s. The damaged or collapsed buildings were mostly constructed using stone masonry bearing wall systems with a maximum of 2 storeys. In this construction type, natural stones of various sizes (50-400 mm) were bonded together using a clay binding mortar to form the walls (Figure 14a). Bearing walls varied from 500 to 800 mm in thickness. The buildings were strengthened with horizontal wooden tie beams (wooden belts), which were used at various heights all around the building perimeters (Figure 14b). The vertical distances between two consequent tie beams varied from 500 to 1500 mm. Tie beams were also used at the locations where the walls were connected to the roofing system. Wooden out-of-plane ties ensured the out-of-plane stability of these thick bearing walls (Figure 14c). Wood boards (planks), supported by timber beams, formed the floor/roof diaphragm in these buildings, as shown in Figure 14d. The reinforced concrete and masonry buildings damaged



Figure 13. Typical masonry buildings constructed in the region



Figure 14. Construction details of typical masonry buildings in the region: a) Wall section; b) wooden tie beams c) out of plane ties d) flooring system

during the earthquakes in Turkey are evaluated using a guide [14] published by the Turkish Chamber of Civil Engineers. This evaluation consists of two stages, namely "Evaluation from Outside" and "Evaluation from Inside". The evaluation from outside requires investigation of the partial/total collapse, assessment of the permanent inter-storey drifts, and examination of damage due to soil. Based on this evaluation, if the condition of the structure requires demolition, no further investigations are performed. Otherwise, the evaluation from inside starts and involves categorisation of the cracks based on their location and thickness. At the end of this evaluation, any encountered structural damage may be identified as minor damage (immediate use of structure is permitted), moderate damage (structure can be used after repair or strengthening), or heavy damage (structure requires demolition since repair and strengthening is not economical and feasible). The damage and collapse mechanisms of masonry buildings can be associated with one, or a combination, of the following failure modes: vertical cracks and splitting at corners, wedge-

shaped corner failures, diagonal cracking on walls, out-of-plane splitting of walls, and the separation of walls from flooring/roofing systems. Observations made in the region related to these types of damage resulting from the Sivrice Earthquake are explained in the following sections, and possible strengthening methods are presented.

4.1. Vertical cracks and splitting at corners

This type of damage occurs due to insufficient interlocking between connecting bearing walls at corners. Examples of this type of damage in the region were seen in two buildings, as shown in Figure 15. It was discovered that the building in Aktarla village was constructed in the 1960s. There is no date of construction for the building in Doğanyol.



Figure 15. Vertical cracks and splitting at corners

These types of damage can be repaired, in various ways, by local strengthening of damaged wall sections. Stone stitching is a method that consists of removing parts of intersecting walls and replacing them with a new, single large stone, which is used for both walls. This strengthening can be performed at different heights along the separated wall intersection. The introduction of new tie rods/beams (wood, reinforced concrete, or steel) is another method to repair the separated wall sections. Moreover, by tightening these tie rods, the gap between the separated walls can be reduced or even closed [15].

4.2. Wedge-shaped corner failure

Cases of wedge-shaped corner failure were observed during the site evaluations. This type of failure occurs due to inadequate connection details of wooden tie beams used at the corners along the building height and at roof levels. Examples of this type of damage in the region are shown in Figure 16.

This type of failure requires reconstruction of the corner region, and provision for adequate bonding of the newly-added wall element to the existing walls. New ties can also be added to compensate for the loss of monolithic behaviour of the damaged section. Another strengthening method is to introduce

a reinforced concrete column at the damaged corner along the height of the wall. In this method, the remaining portion of the wall is reconstructed using similar stone masonry [15].



Figure 16. Wedge shaped corner failure

4.3. Diagonal cracking on walls

Diagonal cracking due to excessive shear and tensile forces was also commonly observed during the field investigations. The width of these diagonal cracks was very small in some of the masonry buildings; however, the increased width resulted in failure of some of the investigated buildings. Examples of this type of damage in the region are shown in Figure 17.



Figure 17. Diagonal cracking on walls

These cracks can be repaired by injecting fluid cement mortar, cement grout or epoxy-based materials into cracks up to 10 mm wide. The reinforced concrete jacketing of walls from both sides is another method that can be deployed to strengthen heavily-damaged walls having crack widths of more than 10 mm. The partial or complete removal and reconstruction of wall sections can also be performed if the damage is extensive and the integrity of the whole system is in danger [15].

4.4. Out-of-plane splitting of walls

This type of damage occurs when out-of-plane wooden ties do not sufficiently resist the motion of a wall in its out-of-plane direction. Some parts of the wall tumble towards either the outside or the inside of the building. Examples of this type

of damage in the region are shown in Figure 18. The partial or complete removal and reconstruction of wall sections should be performed to repair this type of damage. During the repair process, the damaged section should be supported by temporary shoring [15].



Figure 18. Out-of-plane wall splitting

4.5. Separation of walls from flooring/roofing systems

During the site visit, it was observed that collapsed or heavily damaged buildings mainly suffered from the separation of bearing walls and floor/roof systems. This was due to the lack of proper connections between bearing walls and flooring/roofing systems. Another reason for this type of damage might be the insufficient strength and stiffness of the flooring/roofing systems (flexible diaphragm). Examples of this type of damage in the region are shown in Figure 19.



Figure 19. Failure due to wall separation

Repair of this type of damage begins with the reconstruction of damaged walls. The flooring/roofing system must then be

repaired appropriately to enable uniform motion of the wall and flooring/roofing system during earthquakes. This connection can be provided through provision of new tie beams (wood, reinforced concrete, or steel) at the top of a bearing wall. In this repair method, the existing flooring/roofing system should be tied adequately to the newly-installed tie beams [15].

4.6. Soil conditions (Çevrimtaş village)

During the site visit, special attention was paid to Çevrimtaş village, which is approximately 1 kilometre away from the epicentre of the earthquake. The masonry buildings in this village experienced the greatest damage. A photograph of Çevrimtaş village is shown in Figure 20. For the purposes of this paper, the village was divided into two separate regions, the upper and lower Çevrimtaş. According to information provided by the General Directorate of Mineral Research and Exploration of Turkey [13], the lower village lies on soft soil (very dense sand, hard clay layers and/or soft rock having extensive cracks) right next to the reservoir of Karakaya Dam. The upper village is located on the highlands of the neighbouring hill, and it lies on strong soil (strong and hard rock) [13]. The geological soil formation map of Çevrimtaş village is shown in Figure 21. During the earthquake, almost all masonry buildings in the lower village collapsed, whereas most of the masonry buildings in the upper village did not experience any damage. Some photographs of the various collapsed masonry buildings located in the lower Çevrimtaş village are shown in figures 22 through 25. An example of a typical undamaged masonry building located in upper Çevrimtaş village is shown in Figure 13 (bottom right).



Figure 20. View of Çevrimtaş village

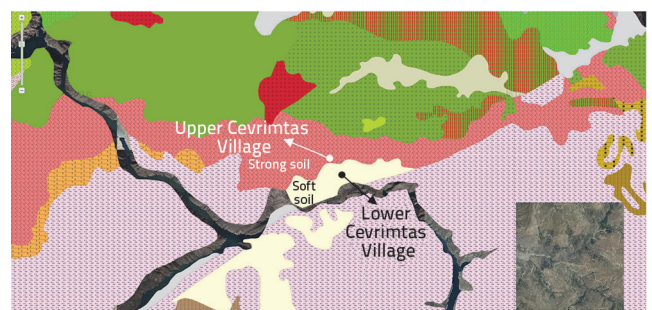


Figure 21. Geological soil formation of Çevrimtaş village [13]



Figure 22. Collapsed masonry building in lower Cevrimtaş village (building 1)



Figure 23. Collapsed masonry building in lower Cevrimtaş village (building 2)



Figure 24. Collapsed masonry building in lower Cevrimtaş village (building 3)



Figure 25. Collapsed masonry building in lower Cevrimtaş village (building 4)

Based on field studies conducted in the area, both liquefaction and lateral spreading were observed along the shorelines of the nearby lake, river, and a dam reservoir (Hazar Lake, Frat

River and Karakaya Dam Reservoir) [16, 17]. Some cracks up to 10 cm wide were also identified on the asphalt road by the reconnaissance team involved in the preparation of this study during their technical visit. However, none of these field studies indicated any liquefaction- or lateral spreading-induced damages in the buildings situated in the earthquake region.

TBEC [12] is used to evaluate the effects of earthquake forces on masonry structures in Turkey. As discussed above, the buildings were constructed on two types of soil: strong and soft soil. The horizontal elastic design response spectrums of these two soil types, which are obtained using TBEC [12], by paying attention to the soil amplification factor, are plotted in Figure 12. The figure indicates the fact that the structures located on soft soil (local site class ZC) are subjected to greater accelerations over a longer period compared to those on strong soil (local site class ZA). Therefore, greater earthquake loads would be exerted on masonry structures constructed on soft soil. This fact related to local site class was believed to be the main reason of collapse of the masonry structures in the lower Çevrimtaş village.

5. Structural damage to mosques

During the field investigations, cases of damage and partial collapse were observed in some of the mosques located in earthquake-affected regions. Mosques usually consist of a dome-like structure covering the main prayer hall and an adjacent tower-like structure (minaret) constructed beside this dome (Figure 26).

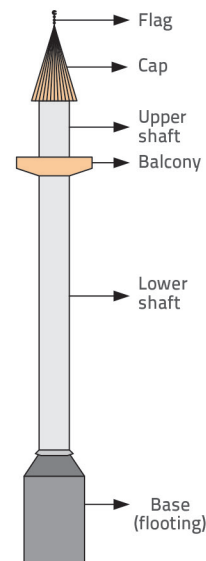


Figure 26. Sections of Minaret

Minarets are slender and tall structures. The bottom of a minaret starts with its base (footing). The lower and upper shafts have a similar cylindrical shape and sit on this footing. A balcony is

located between the lower and upper shafts. The conical tapered spire, called a cap and flag (usually in a crescent moon shape), sits on top of the minaret. The base, shaft sections, and caps of the mosques in the region are usually made of a combination of reinforced concrete and masonry. The caps are made of masonry, and the flags are made of copper, brass, or chrome. The height of a minaret varies based on the height of the adjacent dome structure. Generally, the heights of minarets in the region are approximately twice the heights of the domes. The heights of flags in the region range from 1.2 to 2.2 m, depending on the height of minaret. Various types of damage were observed in the mosques in the region as presented in Table 4. This damage is explained in the following section in detail.

Table 4. Mosque damage types

Name of mosque	Damage type
Yolüstü	Cap collapse
Yeşil Yurt	Flag and cap separation
Furkan	Cap collapse
Sivrice	Heavy damage to structural members
Koçharmanı	Flag and cap separation
Aktarla	Flag and cap separation
Pütürge	Flag and cap separation
Koldere	Upper shaft collapse

5.1. Flag and upper shaft failure

During site investigations, minarets with similar cap damage were observed. During the earthquake, the tapered section of the cap could not resist lateral loads produced by the motion of the flag. As a result, the flag and some parts of the cap detached from the remaining part of the cap. The failure plane usually passed through the mortar interface between the bricks where the weakest plane was located. The photographs related to this type of damage are shown in Figure 27.



Figure 27. Damage to minarets due to separation of flag from cap

This type of failure does not produce any damage to the surrounding area when the flag is not fully detached from the cap and does not fall off. However, when they are detached, significant damage can be observed due to the debris falling from the minaret. This type of damage was observed in some of the mosques in the region, as shown in Figure 28. In Koldere village, the earthquake resulted in the collapse of the flag, cap, and upper shaft of the minaret, and the debris fell down into the main prayer hall of the mosque. The roof of the mosque was punched through due to the falling debris and the mosque suffered severe damage. This type of failure may be experienced due to the discontinuity in stiffness since the upper shaft is usually constructed with a smaller area compared to the area of the lower shaft. Another reason may be the effect of the second vibration mode since the upper shaft is exposed to lower compressive stress compared to that of the lower shaft. The flag and some parts of the cap of Yolüstü and Furkan Mosques also collapsed and fell down. The cars parked on the street were damaged due to the falling debris of Yolüstü Mosque; however, the debris did not result in any other damage to the Furkan Mosque.



Figure 28. Damage due to falling debris

These types of damage and failure of minarets will be observed in future earthquakes unless they are strengthened. Fibre reinforced polymers can be used to repair and strengthen masonry minaret structures against shear and bending stresses [18, 19]. In new constructions, these damages may be prevented using reinforced masonry along the minaret height.

5.2. Reinforced Concrete Mosque (Sivrice)

The Sivrice Mosque was built in 2000 using reinforced concrete and it experienced heavy damage during the earthquake. There were shops at the ground floor level of the structure; the mosque was located on the first storey. There was little or no damage at the shop level; however, the mosque section of the building experienced severe damage. Photographs of the damaged mosque are shown in Figure 29. A closer view of a damaged column is also shown in this figure. Based on visual



Figure 29. Sivrice Mosque after the Earthquake

observations made at the site, the reasons for damage were associated with poor quality of concrete, use of undeformed (plain) reinforcing bars, and insufficient use of transverse reinforcements. These deficiencies were believed to be a result of inadequate inspection of the construction process, since structural design of the building was based on a very detailed and comprehensive code, Turkish Earthquake Code (TEC) [20], which was in effect at that time. TEC [20] prohibited the use of any concrete having compressive strength of less than 20 MPa; it required the use of deformed reinforcing bars, and enforced the use of adequate transverse reinforcements, especially in the confinement zones of column and beam ends. The minaret of this mosque was not damaged. However, due to structural damage observed in the mosque, it had to be demolished one week after the earthquake.

6. Conclusions

Based on the site observations, the following conclusions can be made:

- Low quality masonry buildings experienced the following damage: vertical cracks and splitting at corners, wedge-

shaped corner failure, diagonal cracking on walls, out-of-plane splitting of walls, and separation of walls from the flooring/roofing systems. These types of damage can be remedied by applying adequate strengthening techniques.

- Based on our current level of knowledge, masonry buildings situated in earthquake regions can be designed and constructed safely. However, the existing structures should be strengthened by appropriate reinforcing techniques.

The knowledge behind the design and construction of good quality masonry structures must be transferred to local masons through proper education and certification. Necessary precautions should be taken while strengthening existing masonry buildings to prevent loss of lives and property in future earthquakes.

- The most common type of damage in minarets was the separation of flags from caps and upper shaft failure. In order to avoid similar earthquake-generated damage and failure, the existing minarets should be strengthened and newly-designed ones should be constructed using reinforced masonry.

Acknowledgments

The authors acknowledge the support provided to the technical team by Atılım University. Special thanks are due to Asst. Prof. Dr. Ceren Demirci Kına and Mr. Tolga Kına for their guidance in Malatya and the Elazığ Representative of Turkish Chamber of Civil Engineers, Mr. Hıdır Kaya, for his guidance in Elazığ. The authors also extend their appreciation to R. Güneş Gökçek for his assistance with the sketches published in this paper.

REFERENCES

- [1] General Directorate of Mineral Research and Exploration (MTA), 2020, <https://www.mta.gov.tr/v3.0/hizmetler/yenilenmis-dirifay-haritalari>, 10.11.2020 (in Turkish).
- [2] Disaster and Emergency Management Authority (AFAD): Preliminary Evaluation Report of January 24, 2020 M_w 6.8 Sivrice (Elazığ) Earthquake, Turkish Ministry of Interior, Department of Earthquake, Ankara, Turkey, 2020 (in Turkish).
- [3] Disaster and Emergency Management Authority (AFAD), <https://www.afad.gov.tr/elazig-ve-malatyada-iyilestirme-calismalari-devam-ediyorkampanya>, 10.11.2020, Turkish Ministry of Interior, Department of Earthquake, 2020 (in Turkish).
- [4] Okay, A.I., Zattin, M., Cavazza, W.: Apatite fissiontrack data for the Miocene Arabia-Eurasia collision, *Geology*, 38 (2010), pp. 35-38.
- [5] Arpat, E., Şaroğlu, F.: The East Anatolian Fault System: Thoughts on its development, *Bulletin of the Mineral Research and Exploration*, 78 (1972), pp. 1-12.
- [6] Herece, E.: The Atlas of North Anatolian Fault Lines, General Directorate of Mineral Research and Exploration, MTA, Special Publication Series-13. Ankara, Turkey, 2008 (in Turkish).
- [7] Şaroğlu, F., Emre, Ö., Boray, A.: Turkey's Active Fault Lines and their Seismic Behaviours, General Directorate of Mineral Research and Exploration, MTA, Report No: 8174, Ankara, Turkey, 1987 (in Turkish).
- [8] Disaster and Emergency Management Authority (AFAD), <https://tdth.afad.gov.tr/>, 10.11.2020, Turkish Ministry of Interior, Department of Earthquake, 2020 (in Turkish).
- [9] Aksoy, E., <https://www.aa.com.tr/turkiye/depemin-merkezinde-yuzey-kiriklari-inceledi-/1727259>, 10.10.2020 (in Turkish).
- [10] Mertol, H.C., Akış, T., Tunç, G.: 24 January 2020 dated Sivrice-Elazığ, Earthquake Report, Civil Engineering Department of Atılım University, Ankara, Turkey, 2020 (in Turkish).

- [11] Pousse-Beltran, L., Nissen, E., Bergman, E.A., Cambaz, M.D., Gaudreau, E., Karasozen, E., Tan, F.Z.: The 2020 M_w 6.8 Elazığ (Turkey) earthquake reveals rupture behaviour of the East Anatolian Fault, *Geophysical Research Letters*, 47 (2020) 13, e2020GL088136.
- [12] Republic of Turkey Ministry of Environment and Urban Planning: TBEC-Turkish Building Earthquake Code, Ankara, Turkey, 2018 (in Turkish).
- [13] General Directorate of Mineral Research and Exploration (MTA) 2020, <http://yerbilimleri.mta.gov.tr/anasayfa.aspx>, 10.11.2020 (in Turkish).
- [14] IMO (Turkish Chamber of Civil Engineers): Damage Evaluation of Reinforced Concrete and Masonry Buildings Subjected to Earthquake Loads, Disaster Preparation and Intervention Committee, Turkish Chamber of Civil Engineers, Ankara, Turkey, 2016 (in Turkish).
- [15] UNDP/UNIDO: Repair and Strengthening of Reinforced Concrete, Stone and Brick-Masonry Buildings, Vienna, 1983.
- [16] Middle East Technical University, Earthquake Engineering Research Centre: The Elâzığ-Sivrice Earthquake [24 January 2020 $M_w=6.8$] Field Observations on Seismic and Structural Damage, Report No: METU/EERC 2020-01, Ankara, Turkey, March 2020.
- [17] Temür, R., Damcı, E., Öncü-Davas, S., Öser, C., Sarğın, S., Şekerçi, Ç.: Structural and geotechnical investigations on Sivrice earthquake ($M_w = 6.8$), January 24, 2020, *Natural Hazards*, 106 (2021), pp. 401–434.
- [18] Valluzzi, M.R., Tinazzi, D., Modena, C.: Shear behaviour of masonry panels strengthened by FRP laminates, *Construction and Building Materials*, 16 (2002) 7, pp. 409-416.
- [19] Shrive, N.G.: The use of fibre reinforced polymers to improve seismic resistance of masonry, *Construction and Building Materials*, 20 (2006) 4, pp. 269-277.
- [20] Ministry of Public Works and Settlement: TEC-Specification for structures to be constructed in disaster areas, Ankara, Turkey, 1998 (in Turkish).